Bovine lactoferricin P13 triggers ROS-mediated caspase-dependent apoptosis in SMMC7721 cells

LIXIANG MENG[1,2], GELIANG XU[1], JIANSHENG LI[1], WENBIN LIU[1],
WEIDONG JIA[1], JINLIANG MA[1] and DECHENG WEI[2]

[1]Department of Hepatic Surgery and Anhui Province Key Laboratory of Hepatopancreatobiliary Surgery,
Affiliated Provincial Hospital of Anhui Medical University, Hefei, Anhui 230001; [2]Department of General Surgery,
Anhui Provincial Children's Hospital, Beijing Children's Hospital Group, Hefei, Anhui 230051, P.R. China

Abstract. Bovine lactoferricin P13 (LfcinB-P13) is a peptide derived from LfcinB. In the present study, the effect of LfcinB-P13 on the human liver cancer cell line SMMC7721 was investigated *in vitro* and *in vivo*. The results of the present study indicate that LfcinB-P13 significantly decreased SMMC7721 cell viability *in vitro* (P=0.032 vs. untreated cells), while exhibiting low cytotoxicity in the wild-type liver cell line L02. In addition, the rate of apoptosis in SMMC7721 cells was significantly increased following treatment with 40 and 60 µg/ml LfcinB-P13 (P=0.0053 vs. the control group), which was associated with an increase in the level of reactive oxygen species (ROS) and the activation of caspase-3 and -9. Furthermore, ROS chelation led to the suppression of LfcinB-P13-mediated caspase-3 and -9 activation in SMMC7721 cells. LfcinB-P13 was demonstrated to markedly inhibit tumor growth in an SMMC7721-xenograft nude mouse model. The results of the present study indicate that LfcinB-P13 is a novel candidate therapeutic agent for the treatment of liver cancer.

Introduction

Hepatocellular carcinoma (HCC) is one of the leading causes of cancer-associated mortality worldwide (1). The primary treatments for liver cancer include surgery, radiation and chemotherapy, however, the success rate of these treatments is limited by toxicity and a high rate of relapse (2). Therefore, the identification of efficient novel treatment methods with low side effect profiles is of high priority in HCC research.

Correspondence to: Dr Geliang Xu, Department of Hepatic Surgery and Anhui Province Key Laboratory of Hepatopancreatobiliary Surgery, Affiliated Provincial Hospital of Anhui Medical University, 17 Lujiang Road, Hefei, Anhui 230001, P.R. China
E-mail: xugeliang2007@sina.com

Antimicrobial peptides (AMPs), which are isolated from a range of organisms, including insects, fish, amphibians and mammals (3,4), are typically cationic and amphipathic molecules (5). AMPs exhibit a wide range of antibacterial activities through direct electrostatic bonding to the anionic surfaces of bacteria, leading to the disruption of their plasma membrane (6). Furthermore, recent studies have reported that AMPs exhibit anti-tumor activity (7-9). This may be because cancer cells contain increased levels of anionic plasma membrane phospholipids compared with normal cells, allowing AMPs to bind and kill cancer cells with increased efficacy (10).

Bovine lactoferricin (LfcinB) is a lactoferrin-derived cationic AMP, which exhibits chemotherapeutic properties in a variety of cancer cells, while demonstrating low toxicity to healthy cells (11). The classical AMP LfcinB is composed of 25 amino acids (FKCRRWQWRMKKLGAPSITCVRRAF) and is limited in its use as a chemotherapeutic due to its high toxicity, poor efficacy and high synthesis cost (7). Therefore, the development of novel AMPs comprised of fewer amino acids and with decreased toxicity is essential for applications in cancer treatment.

In the present study, the novel peptide LfcinB-P13 (KCRRWLKRMKKLG), an analog of LfcinB, was designed and synthesized as an amphipathic AMP of 13 amino acids in length. The effect of LfcinB-P13 on the human HCC cell line SMMC7721 was studied. The results demonstrated that the synthetic LfinB-P13-induced apoptosis in SMMC7721 cells was caspase-dependent and reactive oxygen species (ROS)-mediated.

Materials and methods

Reagents and experimental animals. LfcinB-P13 (KCRRWLKRMKKLG) was synthesized by GL Biochem, Ltd. (Shanghai, China) using stepwise solid-phase peptide synthesis. Sixty male Nude mice (age, 6-8 weeks old; weight, 18-20 g) were obtained from Yangzhou University (Yangzhou, China) and housed in a rodent facility at 22±1℃ with a 12 h light/dark cycle. The mice were provided with continuous standard rodent feed and water for acclimatization. All procedures involving animals and their care were conducted in

accordance with protocols approved by the Ethics Committee of Anhui Medical University (Hefei, China).

Cell culture. Wild-type liver (L02) and HCC (SMMC7721) human cell lines were obtained from the American Type Culture Collection (Manassas, VA, USA) and maintained in RMPI-1640 medium supplemented with 10% fetal calf serum (FBS) (both GibcThermo Fisher Scientific, Inc., Waltham, MA, USA), 100 U/ml penicillin and 100 U/ml streptomycin (both Beyotime Institute of Biotechnology, Haimen, China). Cells were cultured at 37˚C in a humidified incubator with 5% CO_2.

Analysis of cell viability. To evaluate the *in vitro* cytotoxic effect of LfcinB-P13 and LfcinB (GL Biochem, Ltd.) on SMMC7721 and L02 cells, an MTT assay was performed as previously described (8). Cells were harvested and seeded into 96-well plates at a density of $5x10^3$ cells/well in medium containing 10% FBS and incubated at 37˚C overnight. Increasing concentrations (0, 20, 40, 60, 80 and 100 μg/ml) of LfcinB-P13 or LfcinB were added to the cells, which were subsequently incubated for a further 12, 24 or 48 h. Cells were incubated with 5 μg/ml MTT solution for 4 h and the purple formazan crystals formed were solubilized using dimethyl sulfoxide (Beyotime Institute of Biotechnology). The absorbance at 490 nm measured using a microplate reader (Bio-Rad Laboratories, Inc., Hercules, CA, USA). Cell viability was calculated using the following formula: Cell viability (%) = (OD_A / OD_B) x 100. OD_A and OD_B refer to the absorbance at 490 of the experimental and control groups, respectively.

Flow cytometric detection of apoptotic cells. The apoptotic effect of LfcinB-P13 on SMMC7721 cells was detected using an Annexin V-FITC (AV-FITC) and propidium iodide (PI) Apoptosis Detection kit (eBioscience, Inc., San Diego, CA, USA). SMMC7721 cells were incubated at 37˚C with multiple concentrations of LfcinB-P13 (range, 0-60 μg/ml) for 24 h. Treated cells were harvested via trypsin digestion, washed twice with PBS and subsequently used in the AV/PI assay, which was performed according the manufacturer's protocol. Assayed cells were analyzed using a flow cytometer (BD Biosciences, San Jose, CA, USA). AV-FITC signals were measured at 635 nm for excitation and 660 nm for emission, and PI signals were measured at 535 nm for excitation and 615 nm for emission. Cell population fractions in four quadrants were analyzed by performing quadrant statistics using FlowJo (version 7.6; Tree Star, Inc., Ashland, OR, USA) software. Early and late apoptotic cells were observed in the lower and upper right quadrants, respectively. The percentage of apoptotic cells was calculated using the following formula: Apoptotic rate (%) = (number of apoptotic cells / total number of cells observed) x 100.

ROS assay. ROS generation was assessed using 2',7'-dichlorodihydrofluorescein diacetate (DCFH-DA), as previously described (9). SMMC7721 cells were treated with LfcinB-P13 at a number of concentrations (0, 20, 40 and 60 μg/ml) and incubated at 37˚C for 24 h. A total of 30 min prior to the end of the experiment, 50 μM DCFH-DA was added to the cell culture medium. Cells were harvested via trypsin digestion

and ROS production was detected by measuring the fluorescent intensity at 240 nm for excitation and 530 nm for emission using a flow cytometer.

Caspase-3 and -9 activity assay. Activation of caspase-3 and -9 was measured using a Caspase-3 or Caspase-9 Colorimetric Assay kit (BioVision, Inc., Milpitas, CA, USA), according to the manufacturer's protocol. SMMC7721 cells were treated with a number of LfcinB-P13 concentrations (range, 0-60 μg/ml) for 24 h at 37˚C. The treated cells were harvested prior to the preparation of cell lysates using Triton X-100 (Sigma-Aldrich; Merck Millipore, Darmstadt, Germany) as previously described (12). The reaction buffer containing the fluorogenic peptide substrates Ac-DEVD-AMC (caspase-3) or Ac-LEHD-AMC (caspase-9) was added to the cell lysates, which were incubated at 37˚C in the dark for 2 h. Caspase-3 and -9 activation in SMMC7721 cells was measured using the Infinite® 200 PRO (Tecan Group, Ltd., Männedorf, Switzerland) microplate reader at 390 nm for excitation and 500 nm for emission. In addition, groups were pretreated with 5 μM antioxidant, N-acetyl-cysteine (NAC), prior to treatment with LfcinB-P13.

SMMC7721-xenograft mouse model and in vivo LfcinB-P13 administration. SMMC7721 cells were harvested in the logarithmic phase of growth and diluted with normal saline. The cell suspension (0.1 ml; $5x10^7$ cells) was transplanted subcutaneously into the right axilla of each nude mouse. When tumors reached between 100 and 300 mm^3 in size, mice were randomly divided into the following four groups: A control group administered with normal salinand three LfcinB-P13-treated groups (10, 30 and 50 mg/kg body weight). Each group contained six mice. LfcinB-P13 was dissolved in normal saline and filtered through a 0.22 μm filter (EMD Millipore, Billerica, MA, USA) prior to administration by intra-tumoral injection (50 μl) three times a week. Following three weeks of treatment, mice were sacrificed by cervical dislocation 24 h following the final administration and the tumor weights of each group were measured. During the treatment, the tumor volume (TV) of each mouse was measured every three days. TV was calculated using the following formula: TV = ½ x a x b^2. In this formula a and b represent the length and width of each tumor, respectively. The rate of inhibition (%) was calculated as follows: [(A-B) / A] x 100. A and B represent the average tumor weight of the control and LfcinB-P13-treated groups, respectively.

Statistical analysis. Values are presented as the mean ± standard deviation of three independent experiments. A one-way analysis of variance was performed to statistically identify differences between the control and treatment groups, followed by Dunnett's test. GraphPad Prism software (version 5; GraphPad Software, Inc., La Jolla, CA, USA) was used for statistical analyses. P<0.05 was considered to indicate a statistically significant difference.

Results

LfcinB-P13 reduces cell viability in SMMC7721 cells. To determine the cytotoxicity of LfcinB-P13 *in vitro*, the
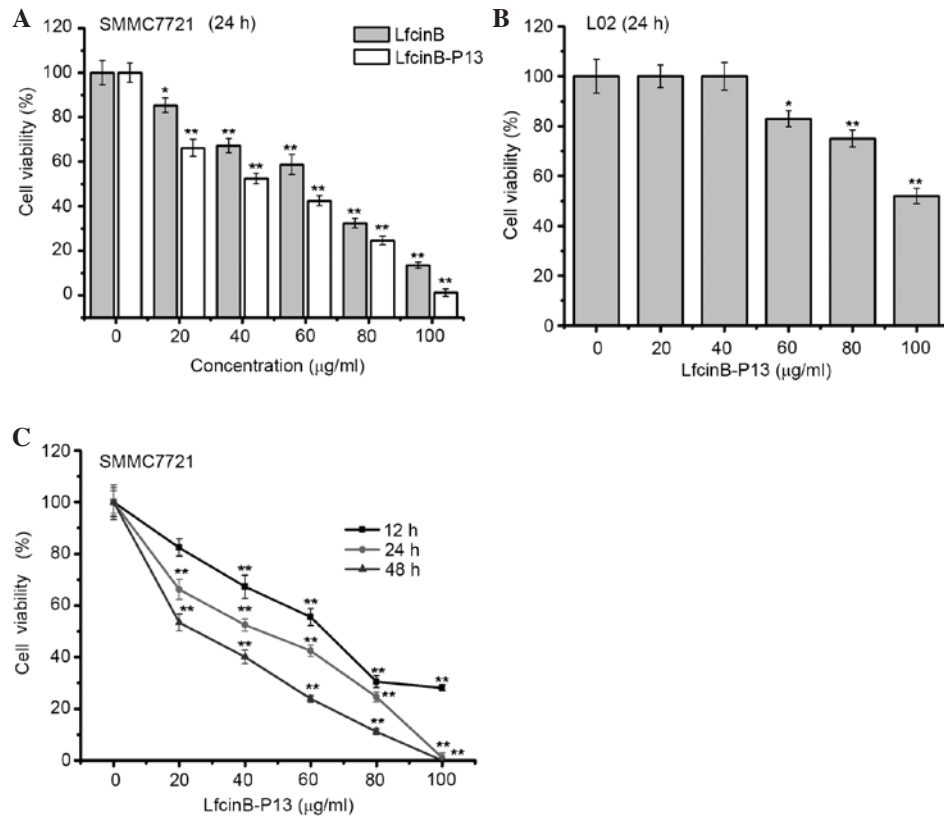
Figure 1. LfcinB-P13 selectively suppresses the proliferation of SMMC7721 cells *in vitro*. (A) LfcinB-P13-treated SMMC7721 cells exhibited decreased viability in a dose-dependent manner 24 h post-treatment. (B) LfcinB-P13 exhibited decreased cytotoxicity in L02 cells 24 h post-treatment. (C) SMMC7721 cell viability was inhibited following treatment with LfcinB-P13 in a dose- and time-dependent manner. Values are presented as the mean ± standard deviation from three independent experiments, each with six replicates. $^{*}P<0.05$, $^{**}P<0.01$ vs. the untreated control group. LfcinB-P13, bovine lactoferricin P13.
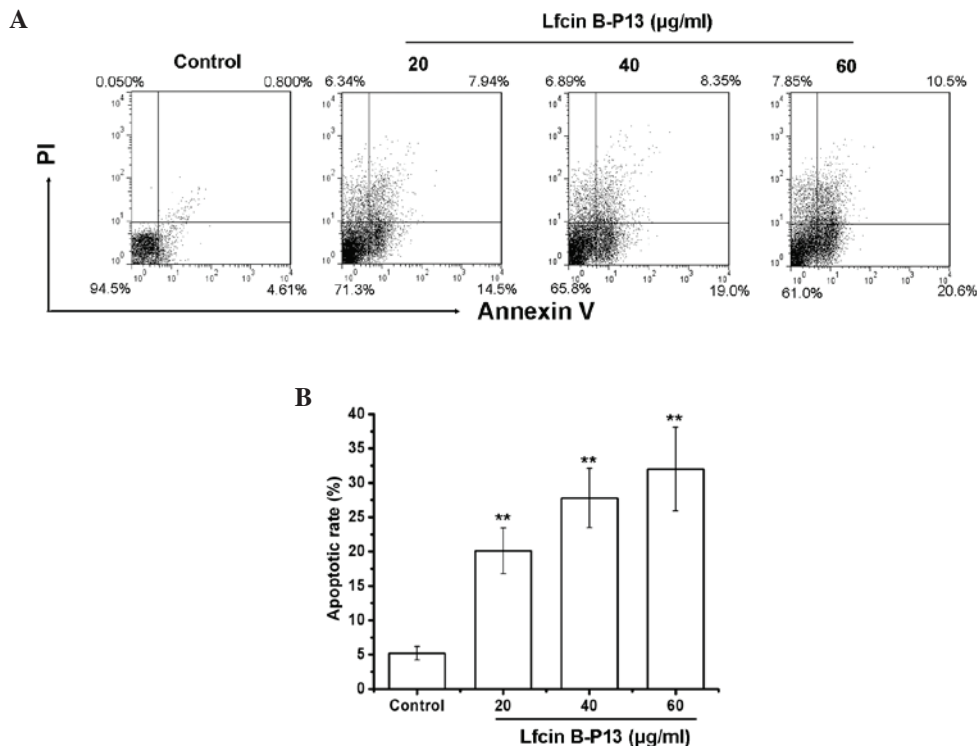

Figure 2. LfcinB-P13 induces apoptosis in SMMC7721 cells. (A) Analysis of apoptosis in SMMC7721 cells was performed using flow cytometry and AV/PI double staining. Late apoptotic cells (AV and PI positive) are in Q2 and early apoptotic cells (AV positive and PI negative) are in Q3. Data points represent the distribution of apoptotic cell populations following treatment with LfcinB-P13 (0, 20, 40 and 60 µg/ml) for 24 h. LfcinB-P13-induced apoptosis in a dose-dependent manner. (B) Percentage of apoptotic cells. Values are presented as the mean ± standard deviation from three independent experiments. $^{**}P<0.01$ vs. the control group. LfcinB-P13, bovine lactoferricin P13; AV, Annexin V; PI, propidium iodidQ, quadrant.

MTT assay was performed. The results of the present study indicated that, following treatment with a number of LfcinB-P13/LfcinB concentrations for 24 h, SMMC7721 cell viability was significantly inhibited in a dose-dependent manner at all doses (P=0.032 vs. the control group; Fig. 1A). Furthermore, LfcinB-P13 notably decreased SMMC7721 cell viability compared with Lfcin-B (Fig. 1A). Treatment of L02 cells, a wild-type human liver cell line, with LfcinB-P13 for 24 h indicated that LfcinB-P13 exhibits a significant cytotoxic effect in L02 cells at 60, 80 and 100 μg/ml compared with the untreated cells (P=0.032, 0.003 and 0.001, respectively; Fig. 1B). Specifically, following 48 h treatment with 80 μg/ml LfcinB-P13, the cell viabilities of SMMC7721 and L02 cells following 48 h were reduced to 24.5 and 75.1%, respectively, suggesting that healthy liver cells are less susceptible to LfcinB-P13 toxicity compared with cancerous cells (Fig. 1B and C). In addition, the inhibition of SMMC7721 cell viability by LfcinB-P13 was dose- and time-dependent (Fig. 1C). The results of the present study demonstrate that LfcinB-P13 has an inhibitory effect on SMMC7721 cell viability *in vitro*.

LfcinB-P13 induces apoptosis in SMMC7721 cells. To determine whether treatment with LfcinB-P13 inhibits the viability of SMMC7721 cells by inducing apoptosis, the percentage of apoptotic cells was measured using the AV/PI assay. Positive staining with AV is associated with the loss of membrane polarity and PI staining is associated with the loss of membrane integrity, which are markers of apoptosis. Therefore, dual staining with AV and PI was used to discriminate between apoptotic and non-apoptotic cells. As demonstrated in Fig. 2A, treatment with LfcinB-P13 induced apoptosis in SMMC7721 cells in a dose-dependent manner. Apoptosis rates were 20.1, 27.8 and 32.1% following treatment with 20, 40 and 60 μg/ml LfcinB-P13, respectively, demonstrating significant upregulation of apoptosis compared with the control group (P=0.0053; Fig. 2B). These results indicate that LfcinB-P13 reduces SMMC7721 cell viability through inducing apoptosis.

LfcinB-P13 increases ROS generation in SMMC7721 cells. Intracellular ROS generation is one mechanism of mediating apoptosis. The results of the present study indicated that ROS levels in SMMC7721 cells were significantly increased following treatment with LfcinB-P13 (P<0.01; Fig. 3A and B). The mean fluorescence intensity in the 60 μg/ml LfcinB-P13-treated cells was increased by 6.58 fold compared with the control group. These results indicate that LfcinB-P13 treatment induces apoptosis in SMMC7721 cells by upregulating ROS generation.

LfcinB-P13 activates caspase-3 and -9 in SMMC7721 cells. Caspase-3 and -9, markers of apoptotic cells, are activated during the early stages of apoptosis. In the present study caspase-3 and -9 were significantly upregulated in the LfcinB-P13-treated cells at all doses compared with the control group (P<0.01; Fig. 4A and B). Treatment with 60 μg/ml LfcinB-P13 increased the activities of caspase-3 and -9 by 6.2 and 5.7 fold compared with the control group. These results suggest that caspase-3 and -9 activation is an underlying mechanism of LfcinB-P13-induced apoptosis.
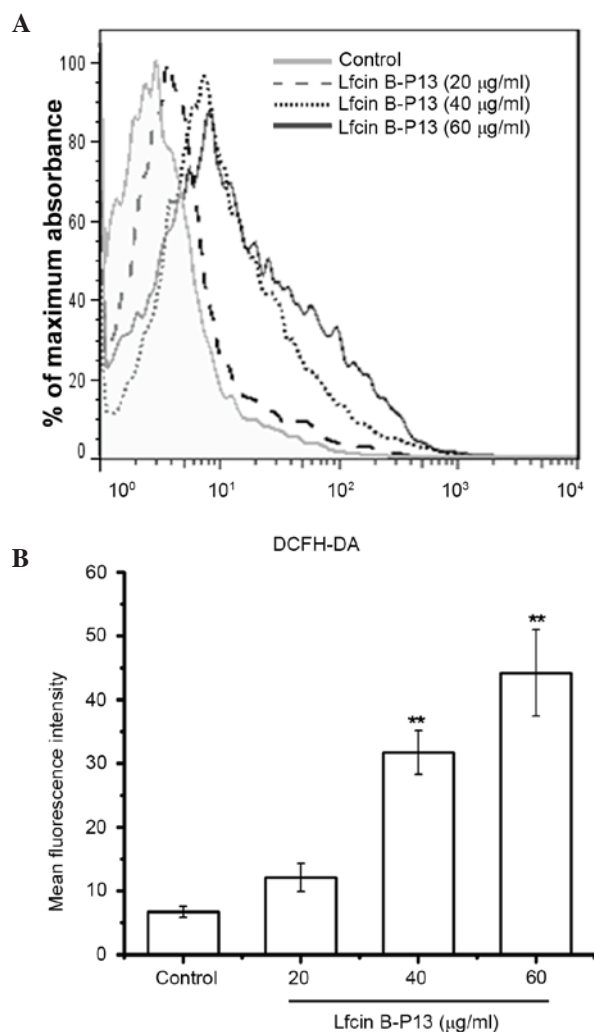

Figure 3. LfcinB-P13 promotes ROS generation in SMMC7721 cells. (A) SMMC7721 cells were cultured in the presence of increasing LfcinB-P13 concentrations (range, 0-60 μg/ml) for 24 h and ROS generation was subsequently evaluated using flow cytometry and the fluorescent probe DCFH-DA. The results shown are the combination of results triplicate experiments. (B) Flow cytometric data was quantified and represented as the mean fluorescence intensity. LfcinB-P13 treatment led to increased levels of ROS in a dose-dependent manner. Values are presented as the mean ± standard deviation of triplicate experiments. **P<0.01 vs. the control group. LfcinB-P13, bovine lactoferricin P13; ROS, reactive oxygen specieDCFH-DA, 2',7'-dichlorodihydrofluorescein diacetate.

LfcinB-P13-induced activation of caspase-3 and -9 in SMMC7721 cells is ROS-mediated. To examine whether LfcinB-P13-induced caspase activity was dependent on ROS, SMMC7721 cells were treated with LfcinB-P13 in the absence and presence of the antioxidant NAC, an ROS scavenger. Fig. 5A and B demonstrate that combined treatment with NAC and LfcinB-P13 significantly decreased activation of caspase-3 and -9 compared with treatment with LfcinB-P13 alone (P<0.01). The results of the present study indicate that upregulated ROS generation is required for LfcinB-P13-mediated caspase-3 and -9 activation.

LfcinB-P13 suppresses tumor growth in SMMC7721-xenografted nude mice. To determine whether LfcinB-P13 prevents SMMC7721 cell growth *in vivo*, a SMMC7721-xenografted nude mouse model was established. These results indicate
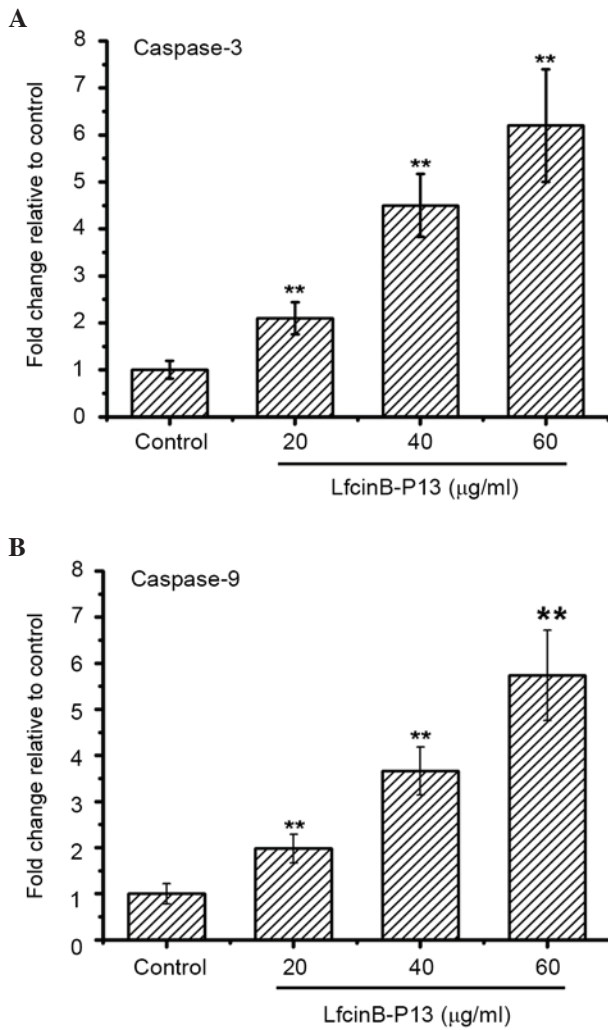
Figure 4. LfcinB-P13 activates caspase-3 and -9 in SMMC7721 cells. Cells were treated with varying concentrations of LfcinB-P13 (range, 0-60 µg/ml) for 24 h. The activities of caspase-3 and -9 were subsequently measured. Treatment with LfcinB-P13 increased the levels of (A) active caspase-3 and (B) active caspase-9 in SMMC7721 cells. Values are presented as mean ± standard deviation of triplicate experiments. **P<0.01 vs. the control group. LfcinB-P13, bovine lactoferricin P13.
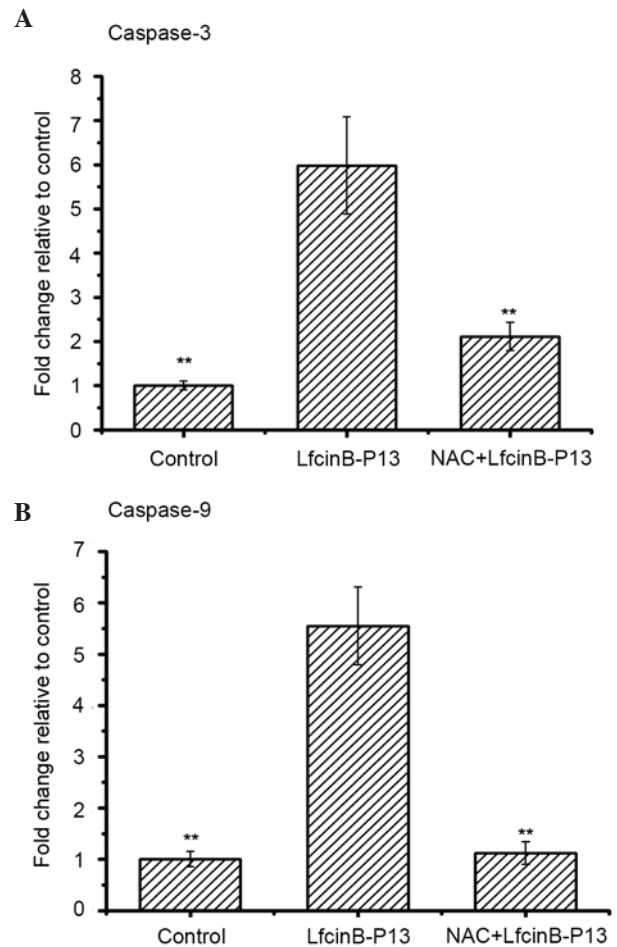
Figure 5. LfcinB-P13-induction of caspase-3 and -9 activity is ROS-mediated. SMMC7721 cells were pre-treated with 5 µM NAC followed by 60 µg/ml LfcinB-P13, treated with 60 µg/ml LfcinB-P13 alone or left untreated (control) for 24 h. (A) Caspase-3 and (B) caspase-9 activity was significantly decreased in the SMMC7721 cells pre-treated with NAC. Values are presented as the mean ± standard deviation of three independent experiments. **P<0.01.

that LfcinB-P13 inhibits SMMC7721 cell growth, in terms of tumor volume and weight, and tumor inhibition rate, in a dose-dependent manner (Fig. 6A-C). Treatment with 30 and 50 mg/kg LfcinB-P13 significantly decreased tumor weight compared with the control group (P=0.006 and 0.005, respectively; Fig. 6B). Tumor inhibition rates were 14.9, 43.3 and 55.8% following treatment with 10, 30 and 50 mg/kg LfcinB-P13, respectively (Fig. 6C).

Discussion

HCC is one of the most common malignancies, is highly metastatic and is the third-leading cause of cancer-associated mortality worldwide (13,14). The majority of traditional chemotherapeutic agents exhibit an extensive profile of side effects, therefore the development of novel drugs with high efficiency and low toxicity is warranted. LfcinB, a lacto-ferrin-derived AMP, is composed of 25 amino acids and has been demonstrated to possess broad-spectrum antimicrobial

activity, in addition to anti-tumorigenic effects (15-17). In the present study, the peptide LfcinB-P13, an analog of LfcinB, was designed and synthesized as an amphipathic AMP of 13 amino acids in length, and the effect of this synthetic compound on SMMC7721 cells was investigated.

The cytotoxic effect of LfcinB-P13 on SMMC7721 and L02 cells was initially investigated. The results of this indicated that LfcinB-P13 significantly inhibits the proliferation of SMMC7721 cells *in vitro*, and that the cells exhibited increased sensitivity to LfcinB-P13 compared with Lfcin-B. The half-maximal inhibitory concentration (IC_{50}) of LfcinB-P13 in SMMC7721 cells was 41.8 µg/ml at 24 h, while the equivalent IC_{50} of LfcinB-P13 in L02 cells was >100 µg/ml, demonstrating increased cytotoxicity in the HCC cell line. The results of this suggest that LfcinB-P13 exhibits cancer-selective activity. The underlying mechanism of LfcinB-P13 action in SMMC7721 cells was subsequently investigated.

Apoptosis is a tightly regulated process of programmed cell death, leading to the elimination of undesirable and defective cells. Induction of apoptosis is a mechanism involved in the action of AMPs (18-20). Dual staining with AV and PI demonstrated that rates of apoptosis were significantly
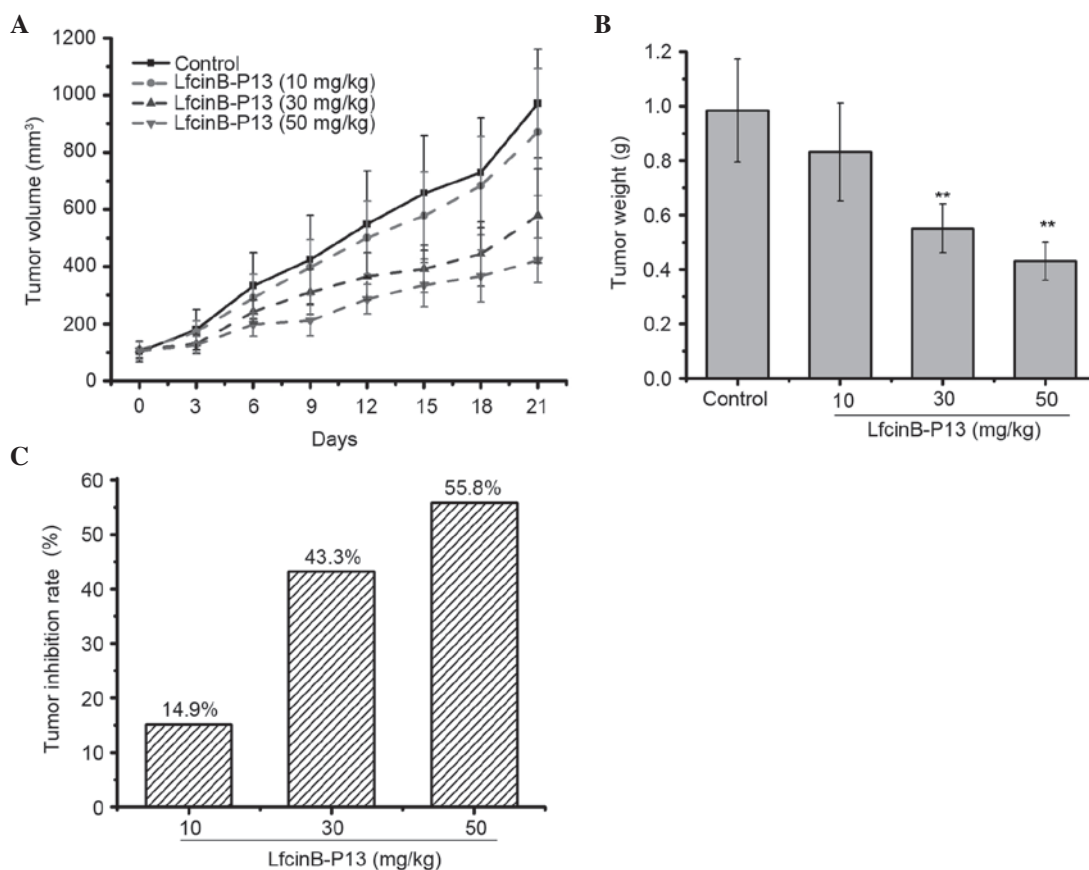
Figure 6. LfcinB-P13 suppresses SMMC7721 cell growth *in vivo*. (A) Tumor volume curve in SMMC7721-xenografted mice treated with or without LfcinB-P13 (10, 30 or 50 mg/kg). Tumor volumes were decreased in the LfcinB-P13-treated cells compared with the control cells. (B) Tumor weight in the treatment groups. (C) Tumor inhibition rate for each treatment group. Groups, n=6. Values are presented as the mean ± standard deviation. **P<0.01 vs. the control group. LfcinB-P13, bovine lactoferricin P13.

increased in cells treated with LfcinB-P13 compared with the control group, suggesting that induction of apoptosis is a mechanism by which LfcinB-P13 prevents the growth of SMMC7721 cells *in vitro*.

ROS, typically regarded as toxic products of cellular metabolism, are able to function as signaling molecules that regulate a number of physiological processes (21). ROS are important in the induction of apoptosis in physiological and pathological conditions. Previous studies have reported that moderate levels of ROS promote cell proliferation and survival (22), whereas excessive levels of ROS induce cell death and lead to ischemia-reperfusion-induced cellular injury, resulting in lipid peroxidation, DNA damage and apoptosis (23,24). In the present study, LfcinB-P13 significantly elevated ROS levels in SMMC7721 cells compared with the control group, which may be the underlying mechanism of LfcinB-P13-induced apoptosis.

Caspase family members serve important roles in the regulation of apoptosis. Caspase stimulation is a marker of apoptotic induction in response to death-inducing signals, which originate from cell surface receptors, mitochondria or the endoplasmic reticulum (25). Caspase-3 and -9 are activated in the early stages of apoptosis, and are therefore frequently used as markers of apoptotic cells (26). Caspase-9 is the primary initiator caspase in the intrinsic pathway of apoptosis (27). Following cleavage and activation of its pro-form, caspase-9 activates caspase-3, which leads to activation of

the apoptotic caspase cascade. In the present study, caspase-3 and -9 were significantly upregulated following treatment with LfcinB-P13 in SMMC7721 cells compared with the control group. Furthermore, it was demonstrated that chelation of ROS by NAC inhibits LfcinB-P13-mediated caspase-3 and -9 activation, suggesting that LfcinB-P13-induced ROS generation is associated with the activation of caspase-3 and -9.

In conclusion, the results of the present study indicate that LfcinB-P13 suppresses the proliferation of SMMC7721 cells *in vitro* and *in vivo* by increasing intracellular ROS generation, which leads to the subsequent activation of caspase-3 and -9, followed by apoptosis. These results suggest that LfcinB-P13 is a novel candidate therapeutic agent for the treatment of liver cancer.

Acknowledgements

References

1. Heindryckx F and Gerwins P: Targeting the tumor stroma in hepatocellular carcinoma. World J Hepatol 7: 165-176, 2015.

2. Wang M, Wang H, Tang Y, Kang D, Gao Y, Ke M, Dou J, Xi T and Zhou C: Effective inhibition of a *Strongylocentrotus nudus* eggs polysaccharide against hepatocellular carcinoma is mediated via immunoregulation in vivo. Immunol Lett 141: 74-82, 2011.

3. Wang G, Mishra B, Lau K, Lushnikova T, Golla R and Wang X: Antimicrobial peptides in 2014. Pharmaceuticals (Basel) 8: 123-150, 2015.

4. Cheung RC, Ng TB and Wong JH: Marine Peptides: Bioactivities and Applications. Mar Drugs 13: 4006-4043, 2015.

5. Tossi A and Sandri L: Molecular diversity in gene-encoded, cationic antimicrobial polypeptides. Curr Pharm Des 8: 743-761, 2002.

6. Sun Y, Dong W, Sun L, Ma L and Shang D: Insights into the membrane interaction mechanism and antibacterial properties of chensinin-1b. Biomaterials 37: 299-311, 2015.

7. Zhang T, Chan CF, Lan R, Li H, Mak NK, Wong WK and Wong KL: Porphyrin-based ytterbium complexes targeting anionic phospholipid membranes as selective biomarkers for cancer cell imaging. Chem Commun (Camb) 49: 7252-7254, 2013.

8. Hilchie AL, Vale R, Zemlak TS and Hoskin DW: Generation of a hematologic malignancy-selective membranolytic peptide from the antimicrobial core (RRWQWR) of bovine lactoferricin. Exp Mol Pathol 95:192-198, 2013.

9. Sheng M, Zhao Y, Zhang A, Wang L and Zhang G: The effect of LfcinB9 on human ovarian cancer cell SK-OV-3 is mediated by inducing apoptosis. J Pept Sci 20: 803-810, 2014.

10. Wang H, Ke M, Tian Y, Wang J, Li B, Wang Y, Dou J and Zhou C: BF-30 selectively inhibits melanoma cell proliferation via cytoplasmic membrane permeabilization and DNA-binding in vitro and in B16F10-bearing mice. Eur J Pharmacol 707: 1-10, 2013.

11. Pieme CA, Guru SK, Ambassa P, Kumar S, Ngameni B, Ngogang JY, Bhushan S and Saxena AK: Induction of mitochondrial dependent apoptosis and cell cycle arrest in human promyelocytic leukemia HL-60 cells by an extract from Dorstenia psilurus: A spice from Cameroon. BMC Complement Altern Med 13: 223, 2013.

12. Rouhollahi E, Zorofchian Moghadamtousi S, Paydar M, Fadaeinasab M, Zahedifard M, Hajrezaie M, Ahmed Hamdi OA, Looi CY, Abdulla MA, Awang K and Mohamed Z: Inhibitory effect of *Curcuma purpurascens* BI. rhizome on HT-29 colon cancer cells through mitochondrial-dependent apoptosis pathway. BMC Complement Altern Med 15: 15, 2015.

13. Dai L, Lei N, Liu M and Zhang JY: Autoantibodies to tumor-associated antigens as biomarkers in human hepatocellular carcinoma (HCC). Exp Hematol Oncol 2: 15, 2013.

14. Yang SF, Chang CW, Wei RJ, Shiue YL, Wang SN and Yeh YT: Involvement of DNA damage response pathways in hepatocellular carcinoma. Biomed Res Int 2014: 153867, 2014.

15. Enrique M, Manzanares P, Yuste M, Martínez M, Vallés S and Marcos JF: Selectivity and antimicrobial action of bovine lactoferrin derived peptides against wine lactic acid bacteria. Food Microbiol 26: 340-346, 2009.

16. Furlong SJ, Mader JS and Hoskin DW: Bovine lactoferricin induces caspase-independent apoptosis in human B-lymphoma cells and extends the survival of immune-deficient mice bearing B-lymphoma xenografts. Exp Mol Pathol 88: 371-375, 2010.

17. Wang S, Tu J, Zhou C, Li J, Huang L, Tao L and Zhao L: The effect of Lfcin-B on non-small cell lung cancer H460 cells is mediated by inhibiting VEGF expression and inducing apoptosis. Arch Pharm Res 38: 261-271, 2015.

18. Park HJ, Choi SY, Hong SM, Hwang SG and Park DK: The ethyl acetate extract of Phellinus linteus grown on germinated brown rice induces G0/G1 cell cycle arrest and apoptosis in human colon carcinoma HT29 cells. Phytother Res 24: 1019-1026, 2010.

19. Tsai TL, Li AC, Chen YC, Liao YS and Lin TH: Antimicrobial peptide m2163 or m2386 identified from *Lactobacillus casei* ATCC 334 can trigger apoptosis in the human colorectal cancer cell line SW480. Tumour Biol 36: 3775-3789, 2015.

20. Pan WR, Chen YL, Hsu HC and Chen WJ: Antimicrobial peptide GW-H1-induced apoptosis of human gastric cancer AGS cell line is enhanced by suppression of autophagy. Mol Cell Biochem 400: 77-86, 2015.

21. Kamogashira T, Fujimoto C and Yamasoba T: Reactive oxygen species, apoptosis, and mitochondrial dysfunction in hearing loss. Biomed Res Int 2015: 617207, 2015.

22. Trachootham D, Lu W, Ogasawara MA, Nilsa RD and Huang P: Redox regulation of cell survival. Antioxid Redox Sign 10: 1343-1374, 2008.

23. Marchi S, Giorgi C, Suski JM, Agnoletto C, Bononi A, Bonora M, De Marchi E, Missiroli S, Patergnani S, Poletti F, et al: Mitochondria-ros crosstalk in the control of cell death and aging. J Signal Transduct 2012: 329635, 2012.

24. Riedl SJ and Salvesen GS: The apoptosome: Signalling platform of cell death. Nat Rev Mol Cell Bio 8: 405-413, 2007.

25. Fiandalo MV and Kyprianou N: Caspase control: Protagonists of cancer cell apoptosis. Exp Oncol 34: 165-175, 2012.

26. Cakir E, Yilmaz A, Demirag F, Oguztuzun S, Sahin S, Yazici UE and Aydin M: Prognostic significance of micropapillary pattern in lung adenocarcinoma and expression of apoptosis-related markers: Caspase-3, bcl-2 and p53. APMIS 119: 574-580, 2011.

27. Würstle ML, Laussmann MA and Rehm M: The central role of initiator caspase-9 in apoptosis signal transduction and the regulation of its activation and activity on the apoptosome. Exp Cell Res 318: 1213-1220, 2012.